Targeted imaging in oncologic surgery : preclinical studies utilizing near-infrared fluorescence and radioactivity

Boonstra, M.C.

Chapter 6

Preclinical evaluation of a novel CEA-targeting Near-Infrared Fluorescent tracer delineating colorectal and pancreatic tumors

MC Boonstra
B Tolner
BE Schaafsma
LSF Boogerd
HAJM Prevoo
G Bhavsar
PJK Kuppen
CFM Sier
BA Bonsing
JV Frangioni
CJH van de Velde
K Chester
AL Vahrmeijer

Int. J. Cancer, 137: 1910–1920. doi:10.1002/ijc.29571

ABSTRACT

Surgery is the cornerstone of oncologic therapy with curative intent. However, identification of tumor cells in the resection margins is difficult, resulting in non-radical resections, increased cancer recurrence and subsequent decreased patient survival. Novel imaging techniques that aid in demarcating tumor margins during surgery are needed. Overexpression of carcinoembryonic antigen (CEA) is found in the majority of gastrointestinal carcinomas, including colorectal and pancreas. We developed ssSM3E/800CW, a novel CEA-targeted near-infrared fluorescent (NIRF) tracer, based on a disulphide stabilized single-chain antibody fragment (ssScFv), to visualize colorectal and pancreatic tumors in a clinically translatable setting. The applicability of the tracer was tested for cell and tissue binding characteristics and dosing using immunohistochemistry, flow cytometry, cell-based plate assays and orthotopic colorectal (HT-29, well differentiated) and pancreatic (BXPC-3, poorly differentiated) xenogeneic human-mouse models. NIRF signals were visualized using the clinically compatible FLARE™ imaging system. Calculated clinically relevant doses of ssSM3E/800CW selectively accumulated in colorectal and pancreatic tumors/cells, with highest tumor-to-background ratios of 5.1±0.6 at 72 h post-injection, which proved suitable for intra-operative detection and delineation of tumor boarders and small (residual) tumor-nodules in mice, between 8 h and 96 h post-injection. Ex vivo fluorescence imaging and pathologic examination confirmed tumor-specificity and the distribution of the tracer. Our results indicate that ssSM3E/800CW shows promise as a diagnostic tool to recognize colorectal and pancreatic cancers for fluorescent-guided surgery applications. If successful translated clinically, this tracer could help improve the completeness of surgery and thus survival.

Novelty and impact statement

This study tends to deliver the first CEA-based clinical relevant tumour-specific near-infrared fluorescent molecular imaging agent that will aid surgical procedures, improve clinical decision making and improve treatment strategies for patients with colorectal or pancreatic cancer. If successful translated, this fluorescent agent, ssSM3E/800CW, enable surgeons to sensitively and specifically visualise cancerous tissue, improving the completeness of surgical resections in recognizing positive resection margins and remnant disease in real-time during surgery or endoscopy and ultimately improve patient survival.

INTRODUCTION

Despite novel therapeutic developments curative surgery is still the cornerstone of cancer treatment. However, positive resection margins are found in up to 27% of rectal cancer patients, and in pancreatic cancer surgery curative resection is achieved in only 10–20% of the patients, resulting in local recurrences and poor overall survival [1,2].

Preoperative tumor detection has improved over the last decade by the introduction of sophisticated techniques such as computed tomography (CT), magnetic resonance imaging (MRI), single-photon emission computed tomography (SPECT) and positron emission tomography (PET) [3]. However, translating information from these images to the operating theatre is difficult due to alteration in body positioning, tissue manipulation by the surgeon and the lack of sensitivity for sub-centimeter lesions. Novel techniques that are able to visualize resection margins in real-time during surgery are necessary to increase the rate of a complete (R0) resections and hopefully survival. Imaging techniques such as SPECT and PET employ a variety of tumor selective peptides or antibodies for tumor recognition. Examples include, biomarkers such as bombesin receptor, integrins, chemokine receptors and adhesions molecules, in addition to 18F-FDG and various radiolabeled monoclonal antibodies, developed initially as therapeutic agents (e.g. cetuximab, bevacizumab, labetuzumab).

Tumor-specific fluorescent-guided surgery uses the same strategy regarding tumor-recognizing tracers but instead of using radioactivity the ligands are conjugated to fluorophores. Tumor-specific peptides are available for a limited number of targets but have the disadvantage that inert conjugation is not readily achieved. Antibodies have the advantage to be available for virtually any target, but their usability is hampered by a long half-life and contamination of the gastrointestinal tract from clearance through the liver and excretion into the bile. Smaller, engineered antibody-derived fragments such as single chain variable fragments (scFvs), can show clear advantages for imaging applications as they display high-level uniform tumor penetration and are rapidly

cleared from the circulation primarily by the kidneys resulting in high tumor-to-background ratios (TBR) and early imaging time points [4,5,6]. Fluorescent-guided surgery has already been demonstrated to be clinically feasible and applicable during surgery using available imaging systems and mainly non-specific contrast agents. Applications include; sentinel lymph-node mapping, tumor imaging, visualization of vital structures and imaging of vascularization and perfusion [7,8].

Carcinoembryonic antigen (CEA or CEACAM5) is a GPI-linked cell surface cell adhesion glycoprotein, which forms part of the immunoglobulin superfamily [9,10]. It is a widely used tumor marker that is abundantly overexpressed on the majority of gastro-intestinal cancers, including colorectal, pancreatic and gastric carcinomas, but has low or restricted expression in normal tissues [9]. CEA has an established potential to facilitate highly specific tumor imaging and drug delivery and is considered a preferred biomarker for colorectal cancer targeting [11]. A variety of approaches have been taken to exploit CEA as a target for cancer imaging. Radiolabeled anti-CEA antibodies and antibody fragments showed clear tumor visualization of human colon tumors using PET imaging in mouse models [6,12,13]. Girgis et al. used a relatively large antibody fragment (110kDa) in a subcutaneous mouse model and clearly demonstrated the potential of CEA-specific antibodies for PET imaging in human pancreatic tumors [14]. Furthermore, phase I trials applying CEA-specific ligands for PET, MRI, or a hand-held gamma-detecting probe show early promise [15,16,17]. Recently, SPECT/CT imaging of patients with colorectal cancer using a 2-step pretargeting system against CEA was introduced [18,19]. The feasibility was shown in a phase I study were the novel approach demonstrated rapid, safe and tumor-specific accumulation [20]. CEA-specific antibodies have also been conjugated to fluorophores for imaging [21-24], but most of these studies are 'proof-of-concept' rather than preparing for introduction into the clinic.

We aimed to develop a clinical translatable CEA-targeted near-infrared (NIR) fluorescent tracer that can be used to visualize tumor-margins and small tumor-nodules *in vivo*. MFE-23, a well-defined scFv [25], was chosen as our starting molecule for engineering because it had showed CEA targeting in a number of pre-clinical studies [26] and, more importantly, in clinical trials [5,15,27] and had been generated as humanized, high affinity variants [28]. We engineered the highest affinity variant to elongate the inter domain linker and create a VH-VL disulfide bond at Kabat positions H44 and L100 respectively, resulting in our targeting agent, ssSM3E, a unique cysteine-stabilized single-chain Fv fragment (ssScFv) that remained homogeneously monomeric. Targeting potential, usability and binding pattern of fluorescent labeled-ssSM3E was evaluated in clinically-relevant orthotopic mouse models of colorectal and pancreatic cancer, using a clinically applicable NIR tracer on Pichia pastoris-expressed ssSM3E, generated with protocols compliant with Good Manufacturing Practices (GMP) [25,29,30]. This CEA targeting tracer is designed, produced and evaluated with the purpose of early clinical translation.

MATERIALS AND METHODS

Single-chain variable (scFv) fragment

Two His-tag containing small antibody fragments were used: a disuphide stabilized anti-CEA ssScFv antibody fragment (ssSM3E) and a control (F73) fragment. The ssSM3E antibody was generated from SM3E, an affinity matured humanized version of MFE-23, [28] by two amino acid substitutions: Gly to Cys and Ala to Cys at Kabat positions H44 and L100, respectively. The chosen locations correspond to that identified as a general site within the scFv framework to stabilize Fvs by disulfide bonds [31].

In addition, the VH-VL linker was extended from (Gly4Ser)3 to (Gly4Ser)4, a strategy we exemplified with humanised MFE-23 [32,33]. Purification of ssSM3E was performed essentially as described before [29,30]. Briefly, protein was directly isolated from Pichia pastoris fermentation broth as a primary capture step; using a radial flow bed (CRIO-MD 62, Proxcys) containing immobilized metal affinity chromatography (IMAC) CellThru beads (Sterogene). Subsequently, the eluted protein fraction was concentrated with a Labscale TFF system (Millipore) using a Biomax 10 kDa ultrafiltration module and subsequently applied to a Superdex 75 size-exclusion column (500 ml bed volume, GE Healthcare) that was equilibrated with PBS (pH 7.4). The fraction containing the monomer ssSM3E was collected and stored at −80°C. The ssScFv control F73 was developed similarly, but an additional amino acid substitution of Tyr to Pro was generated at position 100b (Kabat numbering) to abrogate affinity for CEA; yielding an ssScFv with no specificity for any known protein.

Human cancer cell lines

A total of 14 cancer cell lines were used in this research including 10 colorectal cancer cell lines and four pancreatic cancer cell lines that were cultured in medium as outlined in Table 1. All cell lines were free of Mycoplasma species and were cultured in a humidified incubator at 37°C and 5% CO2. Except for the two high CEA-expressing cell lines used during the *in vivo* experiments, HT-29-luc2 and BXPC-3-luc2, all cell lines were purchased from ATCC but none were authenticated within 6 months before the *in vitro* experiments.

Table 1: CEA expression on ten human colorectal and four pancreatic cancer cell lines

	Human cancer cell lines:			
	Cell-line:	Type[1]:	Culture medium:	CEA expression:
Colorectal	HCT-8	Colorectal (adeno)carcinoma	RPMI1640 + 10% FBS	+
	CACO-2	Colorectal (adeno)carcinoma	DMEM + 20% FBS	+
	HCT-116	Colorectal (adeno)carcinoma	RPMI1640 + 10% FBS	-/+
	HT-29	Colorectal (adeno)carcinoma	RPMI1640 + 10% FBS	++
	RKO	Colon carcinoma	RPMI1640 + 10% FBS	-/+
	COLO-320	Dukes'Type C, colorectal (adeno) carcinoma	RPMI1640 + 10% FBS	-/+
	SW-620	Dukes'Type C, colorectal (adeno) carcinoma, derived from metastatic	RPMI1640 + 10% FBS	++
	LoVo	Dukes'Type C, colorectal (adeno) carcinoma, derived from metastatic site	F12K + 10% FBS	++
	LS-180	Dukes'Type B, colorectal (adeno)carcinoma	DMEM + 10% FBS	++
pancreatic	BXPC-3	(Adeno)carcinoma (primair)	RPMI1640 + 10% FBS	++
	HS766T	(Adeno) carcinoma (Lymphnode metastasis)	DMEM + 10% FBS	++
	MIAPACA-2	(Adeno) carcinoma (primair)	DMEM + 10% FBS	+
	PANC-1	(Adeno)carcinoma	DMEM + 10% FBS	-/+

All evaluated cell lines are from epithelial origin and showed expression of CEA. Five colorectal and two pancreatic cancer cell lines possess high CEA expression (11), while two colorectal and one pancreatic moderate (1) and three colorectal and one pancreatic cell line low expression (1/2). [1]Source: ATCC.org. Abbreviation: FBS: fetal bovine serum.

The BXPC-3-luc2 cell-line was purchased from PerkinElmer (MA, USA) within 6 months prior to the experiments. BXPC-3 (CRL-1687™), provided by ATCC, was used as source for the parental cell line.

The HT-29-luc2 cell-line was established in our own research group as described by Verbeek et al. [34]. The authentication of the cell line before experiments was carried out using the AmpFℓSTR® Identifiler™ PCR Amplification Kit (Applied Biosystems) by BaseClear (Leiden, Netherlands). In short, DNA was isolated using Chemagic Blood250 Special Kit (Chemagen) and the Chemagic Module I. DNA was quantified using Quantifiler™ Real-Time PCR amplification kit (Applied Biosystems). The selected markers included Combined DNA Index System (CODIS) core STR loci (CSF1PO; 5q33.3–34, D13S317; 13q22–q31, D16S539; 16q24-qter, D5S818;5q21–q31, D7S820; 7q, TH01; 11p15.5, TPOX; 2p23-2pter, and vWA; 12p12-pter) and 1 sex Chromosome locus, Amelogenin (Xp22.10–22.3 and Y). The result of the STR profiling was compared to the STR profile for HT-29 present in the ATCC STR profiling database.

Flow-cytometry

HT-29 and COLO-320 were grown to 90% confluence and detached with trypsin/EDTA. After evaluation of cell viability using trypan blue, cells were adjusted to 0.5×10^6 cells/tube in ice cold PBS and incubated with 100 µl of anti-CEA rabbit polyclonal antibody (A0115 DAKO, 1/800), the anti-CEA ssScFv (ssSM3E) or non-specific ssScFv (F73) control on ice for 30 min. After incubation, cells were washed 3 times in ice cold PBS and incubated for the ssScFv fragments (either non-labeled or labeled with 800CW) with an anti-His antibody/Alexa488 conjugate (35310 Qiagen, 1/100) and with goat anti-rabbit fluorescein (4050-02 Southern Biotech, 1/50) for the polyclonal antibody on ice for 30 minutes. After 3 washing steps with ice cold PBS, cells were resuspended in 400 µL PBS containing propidium iodide (PI) to stain dead cells. Samples were measured on the LSRII flow-cytometer (BD Biosciences) and 1×105 living cells were counted.

Functionalization of ssScFv fragments

The CEA-specific fragment was covalently conjugated to biotin using N-Hydroxysuccinimide (NHS) ester chemistry against primary amines following manufacturer protocol (Thermo Scientific, USA). Using the same chemistry, both fragments, ssSM3E and F73, were also conjugated to fluorescein (Sigma-Aldrich, λex= 494 nm, λem= 521 nm) and IRDye800CW (LICOR, USA, λex= 773 nm, λem= 792 nm). In short, the conjugation was performed with a 4-fold molar excess of the NIR dye IRDye800CW to ssSME3, the mixture was incubated and mixtured for 4 hours at room temperature after which the non-conjugated dye was removed using a Zeba Spin Desalting column (Pierce

Biotechnology, Rockford, USA). The conjugation to IRDye800CW resulted in 3 different tracers: the specific (ssSM3E/800CW), control (F73/800CW) and the inactive version of IRDye800CW-NHS (IRDye800CW carboxylate) was used as label alone. Absorbances of the samples were measured at 280nm and 780nm using a spectrophotometer (Pharmacia Biotech, Ultrospec 3000) after which the labelling ratios were calculated using the following formula (following manufacturer protocol): Dye/protein = (A780/εDye)/ (A280−(0.03 × A780)/ εprotein), where the molar extinction coefficient of IRDye800CW (εDye) is 240,000 M−1 cm−1 and for the protein (εprotein) is 48,735 M−1 cm−1.

Human colorectal and pancreatic tissue samples

Randomly chosen paraffin-embedded tumor blocks from 10 colorectal and 10 pancreatic cancer patients were obtained from the pathology department and sectioned. Tumor sections were simultaneously stained for CEA using ssSM3E/biotin or for CEA and CEA-like proteins using the commercially available polyclonal anti-CEA antibody (1/4000, A0115 DAKO). For ssSM3E-biotin, sections were incubated overnight at pre-determined dilutions (1 ug/ml). After 30 min of incubation with Vectastain ABC Kit (Vector Laboratories) sections were visualized using DAB solution (DAKO kit). After incubation of the sections with the anti-CEA polyclonal antibody (1/4000), DAKO envision +HRP anti-rabbit was added for 30 min (K4001; DAKO Cytomation, Glostrup, Denmark) followed by diaminobenzidine solution (DAB+; DAKO kit) to visualize the CEA expression. All sections were counterstained with hematoxylin, dehydrated and finally mounted with pertex. All samples were handled in an anonymous fashion according to the national ethical guidelines ('Code for Proper Secondary Use of Human Tissue,' Dutch Federation of Medical Scientific Societies) and was approved by the Institutional Ethics Committee of the Leiden University Medical Center.

Immunofluorescent cell assay

To evaluate binding capacity of the ssScFv fragments on living cells, tumor cells with high (HT-29) and low CEA expression (COLO-320) were seeded on chamber slides at a density of 40,000 cells per chamber in 200 uL of the corresponding medium. After 72 h, cells were incubated with the fluorescein conjugated anti-CEA polyclonal antibody and various concentrations of the specific (ssSM3E/fluorescein) or control (F73/fluorescein) tracers for 1 h at room temperature. After incubation, cells were washed 2 times with 0.5% BSA/PBS to discard excess non-bound tracers. Cells were incubated with secondary antibodies anti-his/Alexa488 (35310 Qiagen 1/100) for 30 minutes at RT. Slides were washed two times and mounted using Vectashield with DAPI for nucleus staining. Fluorescent signals were detected using a Leica DM5500 B fluorescence microscope.

Cell based plate assay

The retained binding capacity of the ssScFv fragments after conjugation to IRDye800CW was evaluated using a plate assay and competition experiments. High CEA expressing (HT-29) and low CEA expressing (COLO-320) cells were plated in a 96 wells plate at a density of respectively 50,000 and 60,000 cells per well. At 100% confluence, cells were washed and incubated with various concentrations (0–650 nM) of the tracers for 1 h at 37°C. For the competition experiment 50nM of ssSM3E/800CW was simultaneously added to the cells with either 50nM, 500nM or 5000nM unconjugated ssSM3E and incubated for 1 h at 37°C. The cells were washed twice and imaged with the Odyssey NIR scanner (LI-COR Biosciences, Lincoln, Nebraska: focus offset 3 mm; 800-nm channel; intensity 8). Next, cells were permeabilized with a 40/60 mixture of aceton and methanol followed by a washing step and 5 min incubation with ToPro3 (1/1000, Invitrogen), a far red nuclear staining fluorescent dye (642/661nm). The wells were then washed once and again imaged with the Odyssey scanner (focus offset 3 mm; 700-nm channel; intensity 8) to quantify the number of cells in each well. The apparent affinity of ssSM3E/800CW was calculated as recently described by Oliveira et al. [35]. The experiments were performed in duplicate.

Animal models

Six week-old athymic female mice (CD1-Foxn1nu, Charles River Laboratories, Wilmington, MA, USA) weighting between 25 and 35 grams were housed in ventilated cages. Normal pellet food and sterilized water were provided ad libitum. Throughout tumor inoculation and imaging procedures, animals were anesthetized with 4% isoflurane for induction and 2% isoflurane for maintenance. The Animal Welfare Committee of Leiden University Medical Center approved all animal experiments for animal health, ethics, and research. All animals received humane care and maintenance in compliance with the "Code of Practice Use of Laboratory Animals in Cancer Research" (Inspectie W&V, July 1999).

To induce subcutaneous tumors, HT-29 cells were injected at 4 sites on the back (500,000 cells per spot). Tumor growth was monitored using a digital caliper.

Colorectal orthotopic tumors were generated as described by Tseng et al. [36]. In short, subcutaneously growing HT-29-luc2 tumors were harvested, cut in small fragments (approximately 3 mm in diameter), and transplanted onto the cecum using a 6-0 suture. The cecal wall was slightly damaged before transplantation to induce immunoreaction and to facilitate tumor cell infiltration. Orthotopic pancreatic tumors were obtained as previously described by Kim et al. [37]. Briefly, a lateral incision was made to explore the spleen and pancreas, which were both laterally externalized exposing their entire length. A fine needle was passed parallel to the vasculature into the pancreas after which 500,000 BXPC-3-luc2 cells were injected. Following imaging, the mice were sacrificed,

organs were collected, and exposed to evaluate biodistribution pattern, and tumors were snap frozen in −80°C isopentane for histological evaluation. Tumor growth of the orthotopic models was monitored weekly by bioluminescence imaging (BLI) using luciferase transfected cell lines. In brief, 150mg/kg of D-luciferin solution (SynChem, Inc., Elk Grove Village, IL) in PBS was intra-peritoneally injected in a total volume of 50 µL 10 min prior to imaging with the IVIS Spectrum imaging system (PerkinElmer LifeSciences, Hopkinton, MA, USA).

Histology

Frozen tissues were sectioned at 6 µm thickness and fluorescence imaging was performed using the Odyssey NIR scanner. All histologic sections were stained with standard hematoxylin-eosin immunohistochemical staining (H&E). To confirm the presence of HT-29 or BXPC-3 cells, additional sections were stained for anti-human CEA (1/4000, A0115, DAKO) and wide-spectrum cytokeratin (rabbit polyclonal 1/200, Abcam inc., Cambridge, MA, USA). Sections were fixed with acetone for 10 minutes followed by 3 washes with PBS. Primary antibody was incubated for 60 minutes at room temperature. All slides were 3 times washed with PBS and incubated with Envision anti-rabbit (DAKO) for 30 min at room temperature. Subsequently, slides were washed with PBS and immunohistochemical staining was visualized using 3,3-diaminobenzidine. Sections were counterstained with hematoxylin, dehydrated, and mounted with pertex mounting medium.

NIR-fluorescent imaging systems

Real-time NIR-fluorescence measurements and fluorescence-guided resections were performed using the FLARE™ NIR imaging system [38]. The Pearl Impulse small animal imaging system (LI-COR) was used as an in-vivo preclinical reference system to measure NIR-fluorescent signals for bio-distribution analysis and to calculate TBR (tumor-to-background ratios). The specific and control images were normalized and regions of interest were marked. The background signals were extracted from the surrounding tissue that was defines as the (normal) tissue/organ that lies around the tumor. After measuring the signal intensity from the macroscopic images they were divided by each other using the following formula: TBR = mean signal tumor/ mean signal surrounding tissue.

Statistical analysis

For statistical analysis and graphs, GraphPad Prism software (version 5.01, GraphPad Software Inc, La Jolla, California) was used. TBRs were calculated by dividing the tumor specific signal by the signal from the surrounding tissue and are depicted as mean plus standard deviation. A two-way repeated measurement ANOVA using the Bonferroni

correction, was used to assess significance between TBRs from the different groups at all time points. P-values equal or lower than 0.05 were considered significant.

RESULTS

Binding pattern of ssSM3E on human colorectal and pancreatic cancer tissue

Immunohistochemical analysis revealed that the ssSM3E/biotin conjugate bound to 9 out of 10 colorectal carcinomas and 5 out of 10 pancreatic carcinomas. Immunohistochemical staining with an anti-CEA polyclonal antibody showed wide overlap, but with a stronger expression pattern, compared with ssSM3E. The ssSM3E/biotin showed a predominantly membrane staining, mainly on the apical surface, whereas the polyclonal antibody stained both the cytoplasm and the apical surface of the tumors (Figure 1). Especially for ssSM3E, an intra-tumoral increase in staining intensity was observed with the highest expression at the invasive front (Figure 1A). In general, ssSM3E revealed a more heterogenic expression pattern but also less aspecific staining of the stromal compartment compared with the polyclonal antibody (Figure 1B).

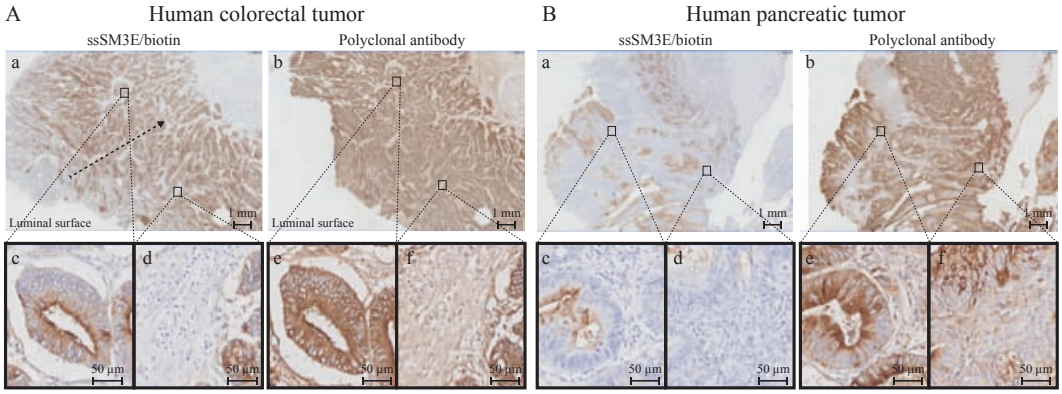

Figure 1 Binding patterns of ssSM3E. (a) Expression in human colorectal tumor sample: ssSM3E/biotin shows a more intense expression at the invasive front compared to the luminal border (a', dashed arrow shows invasive front) which is not seen with the polyclonal antibody (b'). ssSM3E/biotin mainly stained the apical membrane (c') and gives low nonspecific background signal (d) compared to the polyclonal antibody (e', f'). (b) Expression in pancreatic tumor sample: ssSM3E/biotin reveals a heterogenic expression pattern (a') while the polyclonal antibody is more homogeneously expressed (b'). Less cytoplasmic staining (c') and stromal compartment (d') is stained using ssSM3E/ biotin when compared to the polyclonal antibody (e', f').

CEA expression on human cancer cell lines

The expression of CEA was further evaluated by flow-cytometry using the polyclonal antibody on a panel of colorectal and pancreatic cancer cell lines. CEA was present on all cell lines as shown in Table 1 . The control antibody did not bind to any of the cell

lines. Five out of ten colorectal cancer and two out of four pancreatic cancer cell lines showed high CEA expression; two colorectal and one pancreatic cell line had moderate and three colorectal and one pancreatic cell line showed low CEA expression. Based on these data, two highly CEA-expressing cell lines (BXPC-3 and HT-29) were selected and transfected with luciferine-2 for further experiments. After characterization, the DNA-profile of HT-29-luc2 was identical to the published DNA profile of HT-29 by ATCC.

Fragment specificity

The specificity of ssSM3E was evaluated using flow-cytometry, were a dose-dependent signal increase was demonstrated on high CEA expressing cells, and no signals were observed with F73 (non-specific ssScFv control fragment) or with both tracers on the low CEA expressing tumor cells (Figure 2A). Similar results were obtained with the

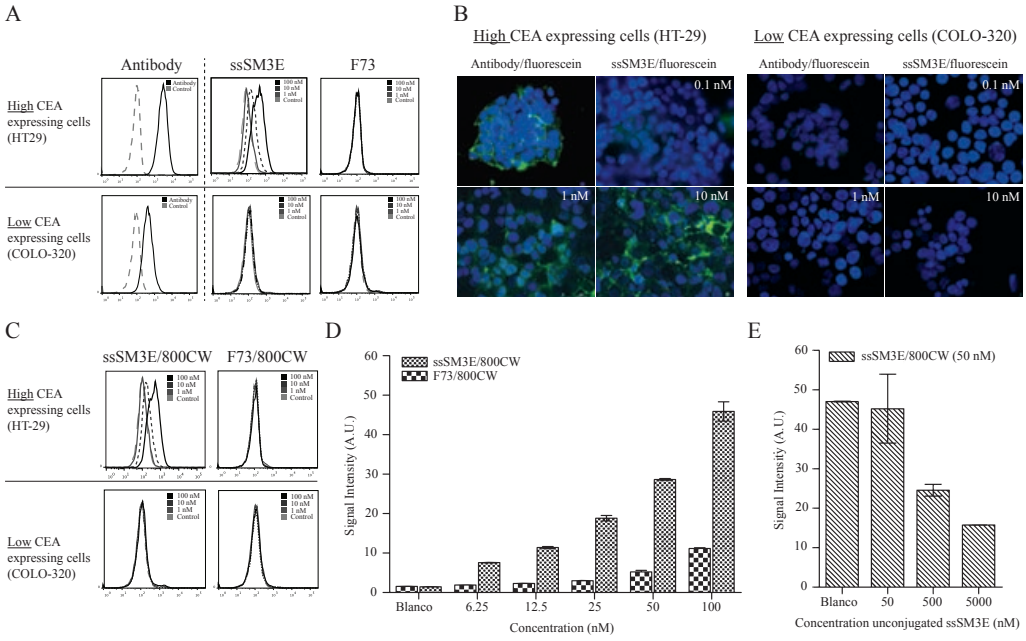

Figure 2 Binding capacity and specificity of the ssScFv fragments. (a) Binding capacity of ssSM3E for CEA using flow cytometry. As positive control, the anti-human CEA polyclonal antibody was used confirming the high and low expression levels of CEA on the tumor cells. Enhancing the concentration of ssSM3E resulted in an increase in signal on the cells with high CEA expression. No signal is observed with F73 or with the negative cell line. (b) High and low CEA-expressing tumor cells were incubated with fluorescein-labeled ssSM3E or fluorescein-labeled polyclonal antibody. An increase in concentration showed higher tumor-specific signal while no signal was observed on the negative cell line. (c) An increase in ssSM3E/800CW showed higher signals from the cells with high CEA expression using flow cytometry while no signal was observed with the control tracer (F73/800CW) or with ssSM3E/800CW on the negative cells. (d) Plate assay analysis showed retained binding capacity of ssSM3E/800CW; increasing the concentration resulted in a nearly linear increase in signal intensity. (e) Competition experiment: a standard concentration of 50 nM ssSM3E/800CW and either 0, 50, 500 or 5,000 nM unconjugated ssSM3E were simultaneously added to CEA-expressing tumor cells. A decrease in fluorescent signal up to 70% of the original signal in the group with the highest dose of unconjugated fragments was observed.

fluorescein-conjugated tracer (ssSM3E/fluorescein) on cells using fluorescent microscopy. Increasing the concentration of ssSM3E/fluorescein resulted in higher fluorescent signals while no CEA-specific signals were observed in the cell-line with low CEA expression (Figure 2B).

NIRF dye conjugation of ssScFv fragments

Both the ssSM3E and the control (F73) ssScFv fragments were labeled with IRDye800CW at mean ratios of 0.92:1 (dye: ssScFv fragment) and 1.08:1 for the specific and control fragments, respectively. Flow-cytometry showed that there were no or minimal alterations in binding specificity of ssSM3E due to conjugation of the fluorescent dyes (Figure 2A and 2C). The retained CEA-specificity of ssSM3E/800CW was confirmed using a cell-based plate assay analysis where an increase in tracer concentration resulted in an almost linear increase in signal intensity, while the control fragment (F73/800CW) showed limited signal intensity only at the highest concentrations (Figure 2D). The same binding assay was used to calculate the apparent affinity (KD) of ssSM3E/800CW which was approximately 15 nM. Competition of ssSM3E/800CW with unlabeled ssSM3E resulted in a 70% reduction in NIR signal intensity, suggesting that the CEA-specific binding capacity of ssSM3E/800CW after conjugation to 800CW is retained (Figure 2E).

In vivo binding characteristics and biodistribution of ssSM3E/800CW

A human colorectal cancer subcutaneous model was used to compare the binding capacity of the tracers and to calculate tumor-to-background ratios (TBR) over time. After tumors were 36mm^2 ± 6, mice were administered with 1 nmol (28µg) ssSM3E/800CW (n=3), F73/800CW (n=3) or 1 nmol (1.2 µg) of non-reactive IRDye800CW-carboxylate (n=3). Using the PEARL small animal imager, tumors could be clearly delineated using ssSM3E/800CW starting at 8 hours after injection until 120 hours. The highest TBR was measured after 72 hours post injection (5.1±0.6) and did not differ significantly from 96 h (4.98±0.6) and 120 h (4.6±0.4). The controls F73/800CW and IRDye800CW showed no or little TBRs at all time points with the highest values (1.4 ± 0.2 for F73/800CW and 1.2 ± 0.1 for IRDye800CW) seen at 24 h (Figure 3A). The differences between ssSM3E/800CW and F73/800CW or IRDye800CW were statistically significant at all studied time-points ($p<0.01$). Using the clinically validated intra-operative FLARE™ imaging system, clear fluorescent delineation was observed in the ssSM3E/800CW group at 24 hours post-injection, while no signal was observed in the control group (Figure 3B). The biodistribution of the ssSM3E/800CW tracer revealed presence of the tracer in the kidneys and the liver, with no accumulation of the tracer in other organs (Figure 3C & 3D).

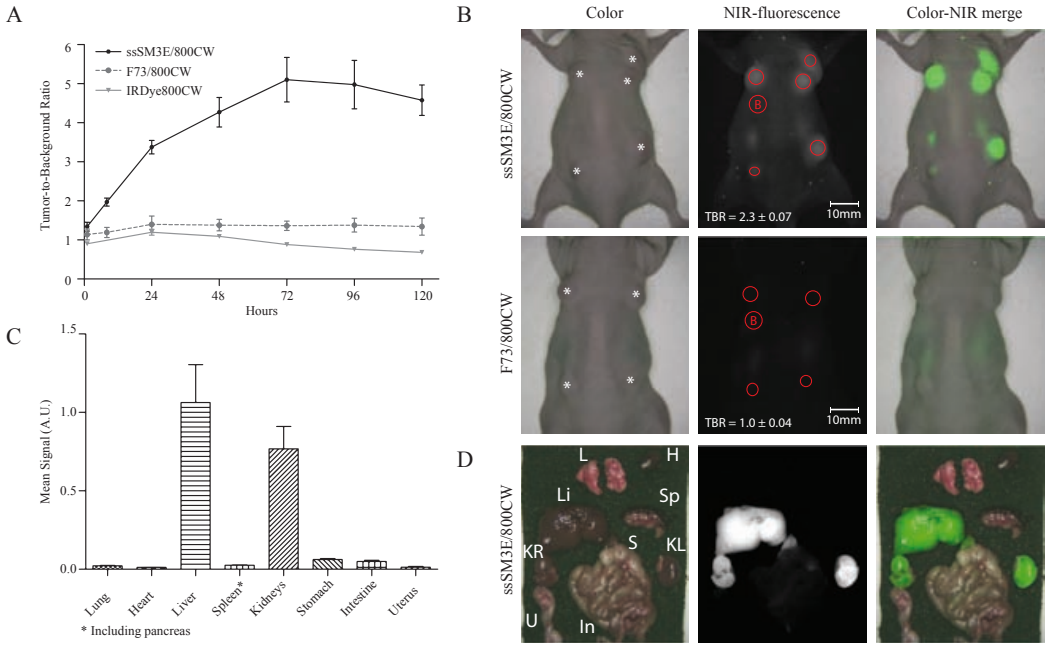

Figure 3 *In vivo* characteristics and biodistribution. (a) TBRs are shown over time. Highest TBR was found for ssSM3E/800CW after 72 hr. (b) Examples of *in vivo* images of mice bearing subcutaneous tumors acquired 72 hr after injection with ssSM3E/800CW or F73/800CW. In red the regions of interest used to calculate TBRs. Mean TBRs were 2.360.07 for ssSM3E/800CW and 1.060.04 for F73/800CW. Both images are normalized and acquired with the FLARE™ system (*tumors of different sizes). (c) Biodistribution of ssSM3E/800CW in multiple organs after 24 hr. Only liver and kidneys show high NIR fluorescent signals owing to the clearance of the tracer. (d) Example of ex vivo images of multiple organs after 24 hr. L: lungs; H: heart; Li: liver; Sp: spleen and pancreas; KR: kidney right; S: stomach; KL: kidney left; U: uterus; In: intestine.

ssSM3E/800CW in orthotopic tumor models

Based on the results from the subcutaneous model, imaging 24 h after tracer administration was chosen as the most optimal and clinically convenient time point to validate the ability of ssSM3E/800CW to bind CEA in more physiologic orthotopic colorectal and pancreatic xenograft tumor models. Bioluminescence was used to estimate the size of the tumors and to confirm tumor specificity by co-localization of the NIR-fluorescent signal from administrated ssSM3E/800CW. Results with the HT-29-luc2 colorectal cancer model (n=3) showed one clear fluorescent nodule after exploration of the abdominal cavity (Figure 4A), whereas the BXPC-3-luc2 pancreatic model (n=4) showed multiple small tumor foci (Figure 4B) and ingrowth in the spleen (Figure 4C). Ex vivo NIR-fluorescence measurements showed tumor specificity of the tracer up-to sub-millimeter sized tumor nodules/ metastasis (Figure 4C). For the orthotopic colorectal model, a mean TBR of 2.55 ± 0.7 was measured using the FLARE™ imaging system and the pancreatic model showed a mean TBR of 2.37 ± 0.4 at 24 hours post-injection (Figure 4D).

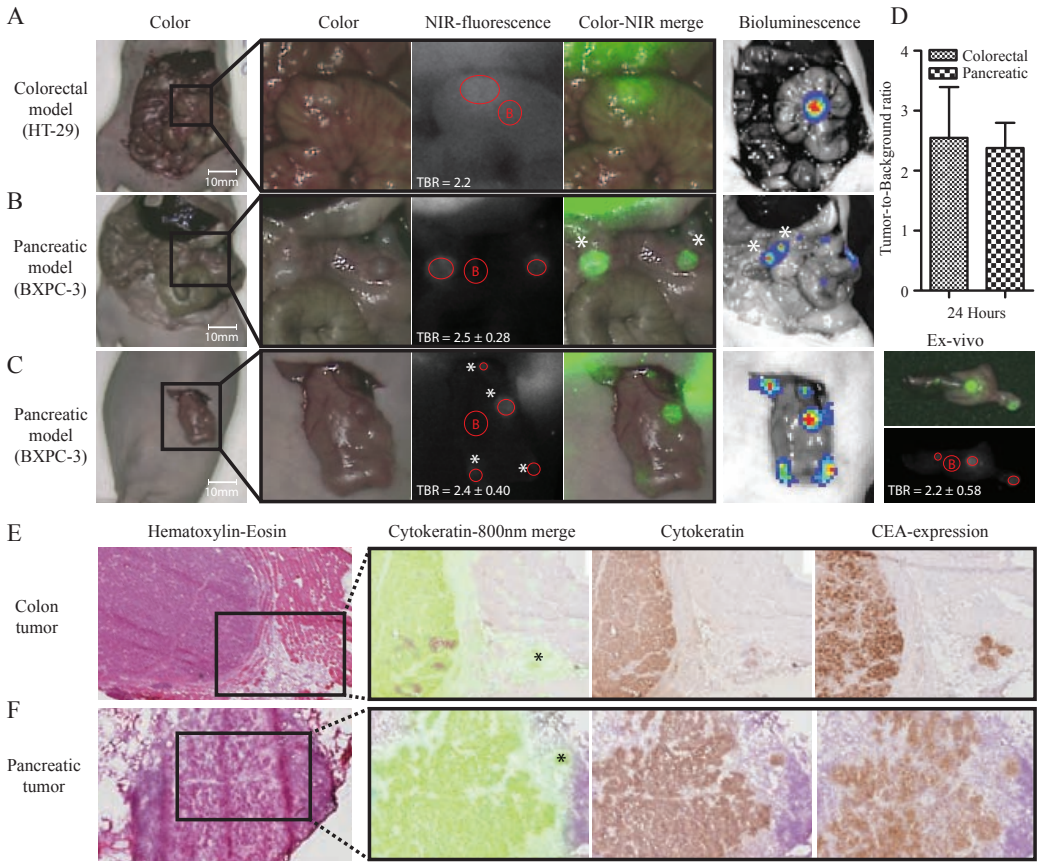

Figure 4 Validating ssSM3E/800CW in orthotopic mice models and histological validation. (a) During abdominal exploration the orthotopic colorectal tumor was found to be NIR fluorescent (TBR of 2.2) and using bioluminescence (BLI) colocalization with tumor cells was confirmed. (b) NIR fluorescent foci in the abdominal cavity were observed in mice injected with BXPC-3 in the pancreas (mean TBR of 2.5±0.28). BLI confirmed that the fluorescent lesions contained human pancreatic tumor cells. (Organs were slightly altered between fluorescent and BLI measurements*). (c) Fluorescent foci in the pancreas (TBR of 2.4±0.40). All fluorescent spots (*) turned out to be tumors using BLI signals. Ex vivo images of the excised spleen and pancreas show three clear millimeter-sized tumor spots (mean TBR52.2±0.58). (d) The orthotopic colorectal model showed a mean TBR of 2.6±0.7 and the pancreatic model a mean TBR of 2.4±0.4 at 24 hr postinjection. All images were acquired with the FLARETM system and are normalized for each model. Colorectal (e) and pancreatic (f) tumors from the xenograft models were evaluated using hematoxylin–eosin (H&E) immunohistochemical staining and NIR fluorescent microscopy. Small tumor foci (*) in the proximity of the primary tumor turned out to be fluorescent. Tumor specificity of the signals was confirmed using additional immunohistochemical stainings for human–cytokeratin and human–CEA. Magnification: x20.

After imaging, excised orthotopic tumors were snap frozen and sliced into multiple sections. Subsequent sections were either imaged for NIR fluorescence or stained immunohistochemically for human cytokeratin/CEA expression in combination with H&E to confirm the presence of human tumor cells. Both colorectal (Figure 4E) and pancreatic (Figure 4F) tumors had high expression of CEA and showed clear similarity between NIR-fluorescent signals, CEA immunohistochemical staining, and localization of the tumor cells. Isolated sub-millimeter sized tumor foci in proximity of the primary tumor were

observed with NIR-fluorescence microscopy and confirmed using additional immunohistochemical staining for cytokeratin and CEA.

DISCUSSION

We investigated a CEA-targeting NIR-fluorescent tracer that proved suitable to identify colorectal and pancreatic tumors in-vivo using real-time fluorescent imaging. The novel tracer showed ability to aid in determining tumor-free resection margins and in recognizing sub-millimeter sized tumor nodules/ metastasis or remnant disease. Thus, the tracer can potentially be applied to the majority of colorectal and pancreatic cancer patients as overexpression is shown in >90% of the colorectal and pancreatic carcinomas [39,40,41]. The current study was purposely performed with a clinically validated ligand, NIR fluorophore, and imaging system to expedite clinical translation. CEA (or CEACAM5) plays a major role in tumor progression and metastasis and show expression disperse the tumor. A recent study that evaluated CEA in comparison to other candidate colorectal cancer markers such as EGFR, TAG-72, and folate receptor-α, showed that CEA was the most sensitive biomarker (93.7 sensitivity) as well as being highly specific (96.1%) when tumor vs normal expression or lymph node expression was assessed [11].

The novel tracer was designed for clinical utility. The antibody fragment we developed for the tracer, ssSM3E, is a disulphide engineered variant of an affinity maturated [28], humanized version of the MFE-23 scFv [25]. MFE-23 was successfully used in two clinical trials for imaging of colorectal tumors, where it was conjugated to radioisotopes and evaluated with either a hand-held gamma-detecting probe or using PET/SPECT imaging [5,15]. Both studies showed accurate tumor localization, high tumor-to-blood ratios with short intervals between injection and imaging and most importantly a lack of significant toxicity. However, MFE-23 is of murine origin so we chose to employ a humanized high affinity variant to address possible immunogenicity. Furthermore, in common with many other scFvs, MFE-23 tended to form concentration-dependent dimers [42], a feature inconsistent with clinical development because of the temporal heterogeneity of product. This we overcame by lengthening the flexible linker and by addition of a VH-VL disulphide (S-S) to generate stable homogeneous monomer anti-CEAs for clinical use. The introduced S-S can also be exploited for chemical modification to facilitate site-specific attachment of ligands or fluorophores as we have demonstrated with similar ssScFvs [33,43].

Bioprocess and reagent suitability were taken into consideration alongside molecular design. The original experimental clinical imaging trials [5,15] with genetically engineered MFE-23 fragments made use of clinical grade scFv using a bacterial expression system. However, ssSM3E can be readily generated in compliance with GMP using a yeast

based production platform. This platform makes use of simple animal free chemically defined media; thereby circumventing safety concerns that are associated with mammalian expression systems (adventitious agents, such as viruses). Furthermore, cells grow at a much faster rate than mammalian cells and genetic manipulation of P. pastoris is relatively easy. The target protein is excreted which allows primary capture to take place by application of the unclarified complete broth directly to a radial flow column [29]. A final product can be generated that has low endotoxin and host cell protein levels and has an excellent safety profile; e.g. MFE-CP was well tolerated in clinical trials at a repeat dosing of 50+ mgs per patient [44].

IRDye800CW is a functionalized NIR-fluorescent fluorophore designed to have optimal *in vivo* characteristics regarding low background fluorescence, low light scattering and high signal-to-noise ratios. Alternatively, fluorophores like the GMP produced ZW800-1, which show similar optical *in vivo* properties, can also be used [45,46]. The fluorophore IRDye800CW is available with a full toxicity report and as a GMP grade product and consequently a clinical grade ssSM3E/800CW can be readily generated [47]. Combined with the knowledge from the previous clinical studies of MFE-23 in humans [5,15,27], which show safety and tumor specificity, the novel ssSM3E/800CW tracer shows promise for rapid clinical development. Nevertheless, before first-in-human feasibility studies can be performed at least an extended single dose intravenous toxicity study must be performed in animals, evaluating the acute toxicity and safety of the tracer. Eventually, phase 3 studies must be designed randomizing between surgery with or without the use of the tracer. When successful, especially for pancreatic cancer patients this will most likely result in a direct increase in patient survival.

The subcutaneous colorectal model used in our study revealed the ability of the tracer to specifically accumulate in tumors with highest TBR at 72 h post injection. The observed relative high signals of the liver may be explained by the lipophilicity and negative charge of 800CW which lead to increased albumin binding and subsequent liver clearance while the probe is mainly cleared through the kidneys [48]. From our experience, a TBR > 2 is sufficient to recognize tumor tissue from the surrounding tissue during surgical procedures in real time. Therefore, an optimal imaging window between 8 h and 96 h post injection could be set. Similarly, Mayer et al. showed, using the non-humanized version MFE-23 conjugated to a nuclear tracer, an optimal window between 24 h and 96 h in colorectal cancer patients [15]. The 24h time-point was chosen as (clinically) the most feasible, therefore, the clinically more relevant orthotopic pancreatic (BXPC-3, poorly differentiated carcinoma) and colorectal (HT-29, well differentiated carcinoma) cancer models were imaged 24 h post injection. Both models successfully showed clear tumor demarcation with mean TBR of approximately 2.5. TBRs from these orthotopic models are slightly lower but are calculated using adjacent normal tissues, which is physiologically more relevant than using non-related tissues or blood, like in subcutaneous models [49].

Two negative controls were utilized, F73/800CW and IRDye800CW alone, which showed no relevant TBRs, confirming the specificity of the in-vivo NIR-fluorescent signals hereby excluding the enhanced permeability and retention phenomenon [50].

A common strategy used to convert animal dose to the human-equivalent-dose (HED) is based on body-surface-area [51]. Using this strategy a HED of ssSM3E/800CW between 0.05 and 0.1 mg/kg can be calculated as a feasible dose for humans. The clinical study that evaluated 125I-MFE-23 used 1 mg total dose, which is considered to be a microdose [52]. A microdosing study limits the costs and investments of the pre-clinical phase (including animal and toxicology studies) and simultaneously provides the ability to generate PK/PD (pharmacokinetic/ pharmacodynamic) data relatively fast [52]. Although microdosing applications lower the translational barrier of novel imaging tracers, appropriate toxicology studies must be designed, in close cooperation with the local medical ethical authorities, which secures the possibility of increasing dose beyond the microdose if necessary. The optimal dose is also dependent on the sensitivity of the imaging system used. There are currently no performance standards and qualifications for the translation of fluorescent imaging systems and the associated targeted tracers [53]. For example, the failure of a tracer to delineate tumors could be interpreted as a failure of the tracer, when in fact the unqualified device was simply not sensitive enough for detection; it is therefore preferred to simultaneously develop novel tracers and imaging systems [53].

To evaluate the number of and select patients who will be suitable for anti-CEA imaging, preoperative evaluation of membrane-associated CEA-expression is important. Selection of eligible colon and rectal cancer patients for clinical studies can be performed relatively straightforwardly with immunohistochemistry on biopsies using the biotin-labeled fragment as shown in this paper. But, for pancreatic tumors this is more difficult due to the general absence of (relevant) biopsies. The advantage of CEA as tumor target above other markers is the broad availability of clinical validated assays to measure soluble CEA levels which potentially could serve as an indicator for CEA upregulation in the tumor tissue. Simeone et al., showed that soluble CEA measured in the sera of 74 out of 81 pancreatic cancer patients (cutoff level 4.8 ng/ml) served as a useful indicator for the presence of pancreatic cancer [40].

The novel anti-CEA tracer, ssSM3E/800CW, presented in our study, has potential to be a highly relevant and translatable tumor-specific agent. It showed clear tumor accumulation and binding pattern in pre-clinical models, generating strong signals that resulted in high contrasts within a wide imaging window. ssSM3E/800CW can aid surgical procedures in recognizing remnant disease, positive lymph nodes, local metastasis and identifying irradical resections making intraoperative frozen section analysis by the pathology department potentially abundant. Furthermore, the NIR fluorescent signals can help the pathologist in recognizing tumor borders and positive (lymph)nodes ex-vivo in the resected specimen while it can also visualize malignant cells with NIR fluorescent

microscopy. The choice of target, appropriateness of molecular design and safety of the ligand will allow rapid clinical development.

REFERENCES

1. Nagtegaal ID, Quirke P. What is the role for the circumferential margin in the modern treatment of rectal cancer? J Clin Oncol. 2008;26:303–312.
2. Stefanidis D, Grove KD, Schwesinger WH, Thomas CR., Jr The current role of staging laparoscopy for adenocarcinoma of the pancreas: a review. Ann Oncol. 2006;17: 189–199.
3. Weissleder R, Pittet MJ. Imaging in the era of molecular oncology. Nature. 2008;452: 580–589.
4. Verhaar MJ, Chester KA, Keep PA, Robson L, Pedley RB, Boden JA, Hawkins RE, Begent RH. A single chain Fv derived from a filamentous phage library has distinct tumor targeting advantages over one derived from a hybridoma. Int J Cancer. 1995;61:497–501.
5. Begent RH, Verhaar MJ, Chester KA, Casey JL, Green AJ, Napier MP, Hope-Stone LD, Cushen N, Keep PA, Johnson CJ, Hawkins RE, Hilson AJ, et al. Clinical evidence of efficient tumor targeting based on single-chain Fv antibody selected from a combinatorial library. Nat Med. 1996;2:979–984.
6. Sundaresan G, Yazaki PJ, Shively JE, Finn RD, Larson SM, Raubitschek AA, Williams LE, Chatziioannou AF, Gambhir SS, Wu AM. 124I-labeled engineered anti-CEA minibodies and diabodies allow high-contrast, antigen-specific small-animal PET imaging of xenografts in athymic mice. J Nucl Med. 2003;44:1962–1969.
7. Vahrmeijer AL, Hutteman M, van der Vorst JR, van de Velde CJ, Frangioni JV. Image-guided cancer surgery using near-infrared fluorescence. Nat Rev Clin Oncol. 2013;10: 507–518.
8. Nguyen QT, Tsien RY. Fluorescence-guided surgery with live molecular navigation--a new cutting edge. Nat Rev Cancer. 2013;13: 653–662.
9. Hammarstrom S. The carcinoembryonic antigen (CEA) family: structures, suggested functions and expression in normal and malignant tissues. Semin Cancer Biol. 1999; 9:67–81.
10. Kuespert K, Pils S, Hauck CR. CEACAMs: their role in physiology and pathophysiology. Curr Opin Cell Biol. 2006;18:565–571.
11. Tiernan JP, Perry SL, Verghese ET, West NP, Yeluri S, Jayne DG, Hughes TA. Carcinoembryonic antigen is the preferred biomarker for *in vivo* colorectal cancer targeting. Br J Cancer. 2013;108:662–667.
12. Vogel CA, Bischof-Delaloye A, Mach JP, Pelegrin A, Hardman N, Delaloye B, Buchegger F. Direct comparison of a radioiodinated intact chimeric anti-CEA MAb with its F(ab')2 fragment in nude mice bearing different human colon cancer xenografts. Br J Cancer. 1993;68:684–690.
13. Lutje S, Franssen GM, Sharkey RM, Laverman P, Rossi EA, Goldenberg DM, Oyen WJ, Boerman OC, McBride WJ. Anti-CEA antibody fragments labeled with [(18)F]AlF for PET imaging of CEA-expressing tumors. Bioconjug Chem. 2014;25:335–341.
14. Girgis MD, Olafsen T, Kenanova V, McCabe KE, Wu AM, Tomlinson JS. Targeting CEA in Pancreas Cancer Xenografts with a Mutated scFv-Fc Antibody Fragment. EJNMMI Res. 2011;1:24.
15. Mayer A, Tsiompanou E, O'Malley D, Boxer GM, Bhatia J, Flynn AA, Chester KA, Davidson BR, Lewis AA, Winslet MC, Dhillon AP, Hilson AJ, et al. Radioimmunoguided surgery in colorectal cancer using a genetically engineered anti-CEA single-chain Fv antibody. Clin Cancer Res. 2000;6:1711–1719.
16. Chester KA, Mayer A, Bhatia J, Robson L, Spencer DI, Cooke SP, Flynn AA, Sharma SK, Boxer G, Pedley RB, Begent RH. Recombinant anti-carcinoembryonic antigen antibodies for targeting cancer. Cancer Chemother Pharmacol. 2000;46(Suppl):S8–S12.
17. Vigor KL, Kyrtatos PG, Minogue S, Al-Jamal KT, Kogelberg H, Tolner B, Kostarelos K, Begent RH, Pankhurst QA, Lythgoe MF, Chester KA. Nanoparticles functionalized with recombinant single chain Fv antibody

fragments (scFv) for the magnetic resonance imaging of cancer cells. Biomaterials. 2010; 31:1307–1315.

18. Aarts F, Boerman OC, Sharkey RM, Hendriks T, Chang CH, McBride WJ, Bleichrodt RP, Oyen WJ, Goldenberg DM. Pretargeted radioimmunoscintigraphy in patients with primary colorectal cancer using a bispecific anticarcinoembryonic antigen CEA X anti-di-diethylenetriaminepentaacetic acid F(ab')2 antibody. Cancer. 2010;116:1111–1117.
19. Schoffelen R, van der Graaf WT, Sharkey RM, Franssen GM, McBride WJ, Chang CH, Laverman P, Goldenberg DM, Oyen WJ, Boerman OC. Pretargeted immuno-PET of CEA-expressing intraperitoneal human colonic tumor xenografts: a new sensitive detection method. EJNMMI Res. 2012;2:5.
20. Schoffelen R, Boerman OC, Goldenberg DM, Sharkey RM, van Herpen CM, Franssen GM, McBride WJ, Chang CH, Rossi EA, van der Graaf WT, Oyen WJ. Development of an imaging-guided CEA-pretargeted radionuclide treatment of advanced colorectal cancer: first clinical results. Br J Cancer. 2013; 109:934–942.
21. Pelegrin A, Folli S, Buchegger F, Mach JP, Wagnieres G, van den Bergh H. Antibody-fluorescein conjugates for photoimmunodiagnosis of human colon carcinoma in nude mice. Cancer. 1991;67:2529–2537.
22. Lisy MR, Goermar A, Thomas C, Pauli J, Resch-Genger U, Kaiser WA, Hilger I. *In vivo* near-infrared fluorescence imaging of carcinoembryonic antigen-expressing tumor cells in mice. Radiology. 2008;247:779–787.
23. Cuesta AM, Sanchez-Martin D, Sanz L, Bonet J, Compte M, Kremer L, Blanco FJ, Oliva B, Alvarez-Vallina L. *In vivo* tumor targeting and imaging with engineered trivalent antibody fragments containing collagen-derived sequences. PLoS One. 2009;4:e5381.
24. Metildi CA, Kaushal S, Pu M, Messer KA, Luiken GA, Moossa AR, Hoffman RM, Bouvet M. Fluorescence-guided Surgery with a Fluorophore-conjugated Antibody to Carcinoembryonic Antigen (CEA), that Highlights the Tumor, Improves Surgical Resection and Increases Survival in Orthotopic Mouse Models of Human Pancreatic Cancer. Ann Surg Oncol. 2014
25. Boehm MK, Corper AL, Wan T, Sohi MK, Sutton BJ, Thornton JD, Keep PA, Chester KA, Begent RH, Perkins SJ. Crystal structure of the anti-(carcinoembryonic antigen) single-chain Fv antibody MFE-23 and a model for antigen binding based on intermolecular contacts. Biochem J. 2000;346(Pt 2):519–528.
26. Sharma SK, Pedley RB, Bhatia J, Boxer GM, El-Emir E, Qureshi U, Tolner B, Lowe H, Michael NP, Minton N, Begent RH, Chester KA. Sustained tumor regression of human colorectal cancer xenografts using a multifunctional mannosylated fusion protein in antibody-directed enzyme prodrug therapy. Clin Cancer Res. 2005;11:814–825.
27. Mayer A, Francis RJ, Sharma SK, Tolner B, Springer CJ, Martin J, Boxer GM, Bell J, Green AJ, Hartley JA, Cruickshank C, Wren J, et al. A phase I study of single administration of antibody-directed enzyme prodrug therapy with the recombinant anti-carcinoembryonic antigen antibody-enzyme fusion protein MFECP1 and a bis-iodo phenol mustard prodrug. Clin Cancer Res. 2006;12: 6509–6516.
28. Graff CP, Chester K, Begent R, Wittrup KD. Directed evolution of an anti-carcinoembryonic antigen scFv with a 4-day monovalent dissociation half-time at 37 degrees C. Protein Eng Des Sel. 2004;17:293–304.
29. Tolner B, Bhavsar G, Foster B, Vigor K, ester KA. Chapter-37: Production of Recombinant Proteins from Pichia pastoris: Interfacing Fermentation and Immobilized Metal Ion Affinity Chromatography. 2012
30. Tolner B, Smith L, Begent RH, Chester KA. Production of recombinant protein in Pichia pastoris by fermentation. Nat Protoc. 2006;1: 1006–1021.
31. Brinkmann U, Gallo M, Brinkmann E, Kunwar S, Pastan I. A recombinant immunotoxin that

is active on prostate cancer cells and that is composed of the Fv region of monoclonal antibody PR1 and a truncated form of Pseudomonas exotoxin. Proc Natl Acad Sci U S A. 1993;90:547–551.
32. Reiter Y, Brinkmann U, Jung SH, Pastan I, Lee B. Disulfide stabilization of antibody Fv: computer predictions and experimental evaluation. Protein Eng. 1995;8:1323–1331.
33. Schumacher FF, Sanchania VA, Tolner B, Wright ZV, Ryan CP, Smith ME, Ward JM, Caddick S, Kay CW, Aeppli G, Chester KA, Baker JR. Homogeneous antibody fragment conjugation by disulfide bridging introduces 'spinostics'. Sci Rep. 2013;3:1525.
34. Verbeek FP, van der Vorst JR, Tummers QR, Boonstra MC, de Rooij KE, Lowik CW, Valentijn AR, van de Velde CJ, Choi HS, Frangioni JV, Vahrmeijer AL. Near-Infrared Fluorescence Imaging of Both Colorectal Cancer and Ureters Using a Low-Dose Integrin Targeted Probe. Ann Surg Oncol. 2014
35. Oliveira S, van Dongen GA, Stigter-van WM, Roovers RC, Stam JC, Mali W, van Diest PJ, van Bergen en Henegouwen PM. Rapid visualization of human tumor xenografts through optical imaging with a near-infrared fluorescent anti-epidermal growth factor receptor nanobody. Mol Imaging. 2012;11: 33–46.
36. Tseng W, Leong X, Engleman E. Orthotopic mouse model of colorectal cancer. J Vis Exp. 2007:484.
37. Kim MP, Evans DB, Wang H, Abbruzzese JL, Fleming JB, Gallick GE. Generation of orthotopic and heterotopic human pancreatic cancer xenografts in immunodeficient mice. Nat Protoc. 2009;4:1670–1680.
38. Troyan SL, Kianzad V, Gibbs-Strauss SL, Gioux S, Matsui A, Oketokoun R, Ngo L, Khamene A, Azar F, Frangioni JV. The FLARE intraoperative near-infrared fluorescence imaging system: a first-in-human clinical trial in breast cancer sentinel lymph node mapping. Ann Surg Oncol. 2009;16:2943–2952.
39. Yamaguchi K, Enjoji M, Tsuneyoshi M. Pancreatoduodenal carcinoma: a clinicopathologic study of 304 patients and immunohistochemical observation for CEA and CA19-9. J Surg Oncol. 1991;47:148–154.
40. Simeone DM, Ji B, Banerjee M, Arumugam T, Li D, Anderson MA, Bamberger AM, Greenson J, Brand RE, Ramachandran V, Logsdon CD. CEACAM1, a novel serum biomarker for pancreatic cancer. Pancreas. 2007;34:436–443.
41. Ieda J, Yokoyama S, Tamura K, Takifuji K, Hotta T, Matsuda K, Oku Y, Nasu T, Kiriyama S, Yamamoto N, Nakamura Y, Shively JE, et al. Re-expression of CEACAM1 long cytoplasmic domain isoform is associated with invasion and migration of colorectal cancer. Int J Cancer. 2011;129:1351–1361.
42. Lee YC, Boehm MK, Chester KA, Begent RH, Perkins SJ. Reversible dimer formation and stability of the anti-tumour single-chain Fv antibody MFE-23 by neutron scattering, analytical ultracentrifugation, and NMR and FT-IR spectroscopy. J Mol Biol. 2002;320: 107–127.
43. Hull EA, Livanos M, Miranda E, Smith ME, Chester KA, Baker JR. Homogeneous Bispecifics by Disulfide Bridging. Bioconjug Chem. 2014
44. Tolner B, Smith L, Hillyer T, Bhatia J, Beckett P, Robson L, Sharma SK, Griffin N, Vervecken W, Contreras R, Pedley RB, Begent RH, et al. From laboratory to Phase I/II cancer trials with recombinant biotherapeutics. Eur J Cancer. 2007;43:2515–2522.
45. Choi HS, Nasr K, Alyabyev S, Feith D, Lee JH, Kim SH, Ashitate Y, Hyun H, Patonay G, Strekowski L, Henary M, Frangioni JV. Synthesis and *in vivo* fate of zwitterionic near-infrared fluorophores. Angew Chem Int Ed Engl. 2011;50:6258–6263.
46. Choi HS, Gibbs SL, Lee JH, Kim SH, Ashitate Y, Liu F, Hyun H, Park G, Xie Y, Bae S, Henary M, Frangioni JV. Targeted zwitterionic near-infrared fluorophores for improved optical imaging. Nat Biotechnol. 2013;31:148–153.

47. Marshall MV, Draney D, Sevick-Muraca EM, Olive DM. Single-dose intravenous toxicity study of IRDye 800CW in Sprague-Dawley rats. Mol Imaging Biol. 2010;12:583–594.
48. Valko K, Nunhuck S, Bevan C, Abraham MH, Reynolds DP. Fast gradient HPLC method to determine compounds binding to human serum albumin. Relationships with octanol/water and immobilized artificial membrane lipophilicity. J Pharm Sci. 2003; 92:2236–2248.
49. Rijpkema M, Oyen WJ, Bos D, Franssen GM, Goldenberg DM, Boerman OC. SPECT- and Fluorescence Image-Guided Surgery Using a Dual-Labeled Carcinoembryonic Antigen-Targeting Antibody. J Nucl Med. 2014;55: 1519–1524.
50. Keereweer S, Mol IM, Kerrebijn JD, Van Driel PB, Xie B, Baatenburg de Jong RJ, Vahrmeijer AL, Lowik CW. Targeting integrins and enhanced permeability and retention (EPR) effect for optical imaging of oral cancer. J Surg Oncol. 2012;105:714–718.
51. Reagan-Shaw S, Nihal M, Ahmad N. Dose translation from animal to human studies revisited. FASEB J. 2008;22:659–661.
52. Scheuer W, van Dam GM, Dobosz M, Schwaiger M, Ntziachristos V. Drug-based optical agents: infiltrating clinics at lower risk. Sci Transl Med. 2012;4:134ps11.
53. Sevick-Muraca EM, Zhu B. The need for performance standards in clinical translation and adoption of fluorescence molecular imaging. Med Phys. 2013;40:040402.